CHALMERS

Preparation of nanostructured NiO particles from waste solutions to remove heavy metal (Pb2+) cations from aqueous solutions

Bachelor Thesis in Nuclear Chemistry & Industrial Materials Recycling

NILENA NILSSON

Chemistry and Chemical Engineering
CHALMERS UNIVERSITY of TECHNOLOGY
Gothenburg Sweden 2015

Abstract

In this study the aim was to recycle Ni from a NiMH-battery waste las NiO nanoparticles by ultrasonic assisted sol-gel process, as well as using recovered NiO nanoparticles for the removal of Pb(2+) cation from aqueous solutions.

For the nanostructured NiO particles produced by ultrasonic assisted sol-gel process on the calcination temperature and duration were investigated, as well as their heavy metal cation (Pb2+) removing capability. X-ray diffractometry was used to determine the crystallite structure and size of the crystallites. Particle size, morphology and chemical composition were studied by scanning electron microscopy (SEM). The Brunaer-Emmet-Teller method (BET) was used to determine the surface area of the nanoparticles and the particle sizes were measured by light scattering particle sizer. Heavy metal removing capability of the nanostructured NiO particles was analysed by inductively coupled plasma optical emission spectrometry (ICP-OES) and Fourier transform IR spectroscopy (FTIR).

Table of Contents

Introduction

Replacement of Ni-Cd batteries in cell phones, video cameras and other portable equipment and tools by Ni-MH batteries or other batteries is needed, since Ni-Cd batteries are not a part of the environmental adjusted battery system [1] and due to the toxic properties of cadmium [2]. When the Ni-Cd batteries were classified as toxic, the nickel-metal hydride (Ni-MH) batteries were invented in 1989. Due to their very high efficiency and the fact that they are rechargeable they are considered to be environmental friendly in today's society. The use of rechargeable batteries has increased all over the world since the 1970s. Ni-MH batteries being one of them and are used as a power source in cell phones, electric vehicles and portable computers for example. A Ni-MH battery has many advantages over many other common battery types, it can be recharged up to 1000 times and the Ni-MH battery lives longer than a Ni-Cd battery [3].

Statistics for sold, collected and recovered materials for Ni-MH batteries are shown in Table 1, where the data is collected from 2009 to 2013. The amount of recovered materials from portable batteries has been increasing over the years and it could be because of new methods invented for the recovery of valuable metals from the battery.

Table 1. Statistics for sold, collected and recovered Ni-MH batteries [4]

Battery statistics Nickelmetallhydride (Ni-MH)					
	Sold 2009 (ton)	Sold 2010 (ton)	Sold 2011 (ton)	Sold 2012 (ton)	Sold 2013 (ton)
Portable batteries	338	567	382	338	349
Industrial batteries	25	158	127	163	203
	Collected 2009 (ton)	Collected 2010 (ton)	Collected 2011 (ton)	Collected 2012 (ton)	Collected 2013 (ton)
Portable batteries	103	244	215	241	275
Industrial batteries	7	1	3	1	2
	Recovered materials 2009 (ton)	Recovered materials 2010 (ton)	Recovered materials 2011 (ton)	Recovered materials 2012 (ton)	Recovered materials 2013 (ton)
Portable batteries	95	222	197	209	247
Industrial batteries	7	1	2	1	1

The Ni-MH contains valuable metals, which are desirable to recycle because the price of nickel is very high. Although the Ni-MH batteries is a recent technology, methods for recycling them are under development [2]. Studies to find new methods to obtain and recycle these waste batteries and the valuable metals they contain, such as nickel, lanthanum and small amounts of other rare earths [5], in them in a good and environmentally friendly way are of great importance. Table 2 presents the nickel price on the market and it is very high, compared to other metals. Nickel is an expensive metal to use but also a valuable metal to recover.

Table 2. Metal prices [6]

Metal	$/kg
Nickel	≈8.10
Copper	≈4.50
Magnesium	≈1.80

The production and consumption of lead (Pb) is increasing all over the world [7]. Since lead is toxic for humans and animals and exposure at trace levels is believed to be enough to create a risk, removing lead from waste water to prevent further contamination, avoid soil pollution or removing it from fresh water, is vital [7].

Metal ions, such as Pb and Cd for example, can accumulate in living organisms causing various diseases and disorders [2]. Lead has been used as an additive in furniture, porcelain, gasoline, paint and other products. It affects the nerve system, especially in young children, and cause blood sepsis and brain disorders. Sweden has suggested to EU that lead should be banned from things that children will be in contact with [8]. Lead poisoning comes from ingestion of food or water contaminated with lead and the different ratios for intake are for food (65%), water (20%) and air (15%) [9].

A lot of different methods and techniques have been developed over the years for removing of heavy metals, such as adsorption, ion exchange and membrane filtration, biological treatment, chemical precipitation and electrochemical technologies [10].

The aim of this study was to try to produce nanoparticles from a solution from leaching of NiMH battery black mass and use the same particles to capture cations of lead (Pb^{2+}). If this works it could be possible to both recycle Ni-MH batteries and use the nanoparticles to remove lead in aqueous solutions and there is a possibility that this method can work for other toxic heavy metals in fresh water and industrial water.

Background

Nickel recycling

The Ni-MH battery system was developed in 1989 and was invented to replace Ni-Cd, because of the toxic properties of cadmium [2]. The need for eco-friendly recycling methods of waste batteries is growing since the amount of batteries has been increasing and the batteries contains a large amount of valuable rare earths [11] and other metals.

There are two process routes for battery recycling, pyrometallurgical and hydrometallurgical. In a pyrometallurgical process the Ni-MH batteries are heated in a high-temperature furnace, the nickel goes to a metallic phase and the rare earths to the oxide form, and the metals are recovered in further processes [5].
Hydrometallurgy recycling gives a metallic compound product, which in some cases needs further treatment. In this recycling method the batteries are dismantled, the anode and cathode materials can be leached separately in acid or base, the metals can then be recovered by precipitation, solvent extraction or electrode position [5].

Removing of heavy metals

Many different techniques for the removal of heavy metals from contaminated water have been developed over the years. Some techniques are: adsorption, ion exchange and membrane filtration, biological treatment, chemical precipitation and electrochemical technologies [10].

The adsorption method with its low costs, high efficiency and ease of operation is one of the major techniques in the removal of heavy metals from water/waste water. The adsorbing capacity depends on the surface area and after years of research a lot of adsorbents are available [12].

Nanosized metal oxides (NMO) such as the magnetic NMOs are very promising as adsorbents. They have high capacity, large surface area and high selectivity. The magnetic type has the ability to be separated from water under a magnetic field and is suitable for recycling and regeneration use [7].

Magnetic nanoparticles, MNP, with their high surface area and magnetic properties makes them very suitable for heavy metal removing. They are also suitable for capturing of microbial pathogens and organic dyes, and they are magnetic and can be reused [10].

Fe_3O_4-GS is a composite material, which combines graphene with the MNP Fe_3O_4. Graphene has; a high contaminant removal efficiency, a large surface area (2630 m^2/g) and a unique structure. With a magnet it is possible to both separate the particles from the aqueous solution and recover and recycle them back to the industrial process [12].

Zeolites, naturally hydrated aluminosilicate minerals, have an exchangeable cation and are used for catching heavy metal cations, such as lead, cadmium, zinc and manganese. Clinoptilolite is the most common natural zeolite and it can be used for the removal of heavy metals from wastewater [13].

Theory

Recovery efficiency

The recovery efficiency is defined as the amount of an element recovered in the final solution compared to its concentration in the original solution. This is expressed as % recovered of the element and calculated as described in Eq. 1.

$$Recovery\ efficiency = 100 \times \frac{(Ci - Cf)}{Ci} \qquad \text{Eq. 1}$$

Where C_i and C_f are the concentrations of the initial and final solutions.

The adsorption capacity

The adsorption capacity is defined as the value of the amount of adsorbed substance reached in a saturated solution. This is expressed as the adsorption amount of heavy metal ions at equilibrium calculated as q (mg/g).

$$q = \frac{C_i - C_f) \times V}{m} \quad \text{Eq. 2}$$

Where C_i and C_f are the concentrations of the metal in initial and final solutions. V is the volume of solution (ml) and m is the weight of the adsorbent (g).

Experimental

Solution-sol-gel (Sol-gel process)

A sol-gel is a molecular solution, which is converted by a chemical reaction to a sol, which reacts further to form a gel intermediate. In the process to form particles of metal oxides, the molecular solution reacts with an alkoxide, which is pure or dissolved in water, and the corresponding metal oxide is formed by heat treatment.

$$M^N(OR)_n \xrightarrow{H_2O,solvent} M^N(OH)_n \xrightarrow{\Delta T} M_2^N O_n$$

In the first step the formation of the gel starts from a homogeneous solution on a molecular level. The second step represents a solidstate reaction [14].

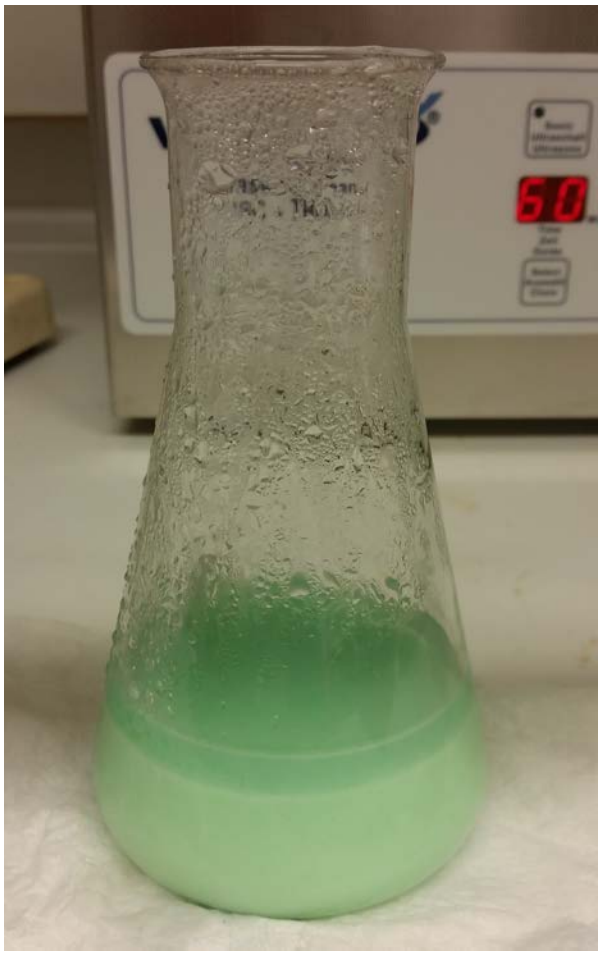

Figure 1. Stratified produced nanoparticles from sol-gel process

X-Ray Diffraction (XRD)

XRD Bruker D8 Advance

XRD is an important technique for the characterization of materials. It uses the interaction of high-energy electromagnetic radiation, x-rays with the electrons in atoms (the so called diffraction of X-rays) to determine crystal structures of crystalline materials. XRD also analyses and gives the crystallite size, which gives information about both crystalline and non-crystalline (amorphous) materials. [15].

Particle Size Analyser

PS Brookhaven Instruments Corporation, BI-90 particle sizer instrument

The Particle Size Analyser is used for analysing mostly nanoparticles but also colloidal-sized materials in non-absorbing liquids to determine the particle size and the diameter of the particles. The aqueous sample is diluted and placed in a special disposable volume cuvette and very small amounts are needed for one analysis, about 50µL to 10 µL. Dynamic Light Scattering, DLS, is used to analyse the sample via a laser. The laser is shot through a polarizer and into the sample, and when the light hits the small particles of the sample the light scatters in all directions. By using a laser the scattering intensity fluctuates over time. The scattered light then goes through a second polarizer where it is collected and analysed and then the results are sent to a screen. The size range that can be measured is 2 nm to 6 µm, depending on the refractive index and concentration of the

sample. This method offers the opportunity of reproducibility and every sample is recoverable after the analysis [16].

Scanning electron microscopy (SEM)

Scanning electron microscopy FEI Quanta 200nFEG ESEM

Scanning electron microscopy uses a high energy electron beam and achieves high-resolution (around 1 nm) images due to the short wavelengths of electrons. The electron beam interacts with the sample surface and this leads to a variety of signals, such as backscattered electrons, secondary electrons and x-rays. This analysis gives a lot of information about the morphology, chemical composition, phase and the crystallography of the sample. It is also used to detect and analyse the micro structure of solid materials [17].
The SEM shows a 3D picture of the samples and gets a bigger picture of the structure of the nanoparticles, if they are agglomerated or not, and which particle size are the smallest.

Brunauer-Emmett-Teller theory (BET)

BET Micromeritics ASAP 2020 Surface Area and Porosity Analyzer

The BET method is used for measuring the surface area, porosity and nanoparticle size, volume and pore size of the sample by allowing a gas adsorb on the surface and measure the multilayer adsorption as a function of relative pressure.
Before the experiment starts the sample is prepared by heating at vacuum pressure, which removes adsorbed molecules and/or gases from the sample so it is clean. A small amount of test gas (for example nitrogen or argon) is then allowed in the system and adsorbs to the sample surface, the test gas flow is increased over time until no more gas adsorbs on the surface [18]. All measurement data from the experiment is calculated to surface, for example surface area, pore size, porosity volume etc.

Inductively coupled plasma optical emission spectrometry (ICP-OES)

ICP-OES, ICAP 6500, Thermo Fischer

The Inductively coupled plasma optical emission spectrometry is an elemental chemical analysis, which uses a plasma and an inert gas, supported with an electromagnetic field by a RF Generator, to analyse the sample. The plasma source is supplied by electric currents which are produced by electromagnetic induction and by time-varying magnetic fields. The plasma electron temperatures have a range between 60000-10000 K, and its high energy makes it possible for it to atomize, ionize and excite all elements in the periodic table. Due to this the ICP-OES shows basically every element in the sample which makes it a very good quantitative method with careful calibration [19].
The concentration of metals in aqueous solutions obtained in the experiments were determined using ICP-OES.

Thermogravimetric Analysis (TGA)

TA TGA Q500 Instruments

The thermogravimetric analysis shows the change in sample weight (%) as a function of temperature. The apparatus is a scale that measures the weight of the sample while changing the temperature over a certain amount of time. When the weight changes, a reaction has occurred at a specific temperature, and the reaction is completed and the system is stabilised when the temperature increases without any change in the sample weight.

Fourier transform infrared spectroscopy (FTIR)

Perkin Elmer Spectrum Two FTIR

The Fourier transform infrared spectroscopy is a method that utilises the interactions between infrared radiation and the chemical bonds in molecules in a sample for identification of the chemical species present in the sample. The sample is placed between an interferometer and a detector for the analysis. The sample then absorbs certain wavelengths, and the spectrum is spread into its component wavelengths and each wavelength is directed into one detector element and the interferogram loses intensity at those wavelengths. The Fourier transform is used to transform the data into a spectrum. A great advantage with this method is that signal-to-noise improves since the whole sample is analysed [20].

Production of nanoparticles

The Nickel solution used in this experiment came from dissolution of an anode from NiMH battery waste. The nickel was extracted from the high concentration chloride medium (aqueous solution) by a solvent-extraction process using Cyanex 923 as extractant dissolved in Solvent 70 [21].

An ultrasonic water bath was used for the preparation of NiO nanoparticles by the sol-gel process. Solutions with different concentrations of $NaHCO_3$ were prepared by dissolution of weighed amounts of $NaHCO_3$ in 100 ml of water. The $NaHCO_3$ was weighed and mixed with water on a heater with a magnetic stirrer until the temperature of 60°C was reached and the pH was checked. Then each of these solutions was added to a 25 ml samples of the Ni-MH waste solution (Table 3) and the beakers placed in the ultrasonic water bath as shown in Figure 2.

Table 3. Sample solution identification, concentration of Nickel, concentration of $NaHCO_3$ and pH in the samples

Sample	Concentration of Nickel solution (g/L)	Concentration of $NaHCO_3$ solution (M)	pH
1	1.875	1.00	6.3
2	1.875	1.50	7.6
3	1.875	1.96	8.0

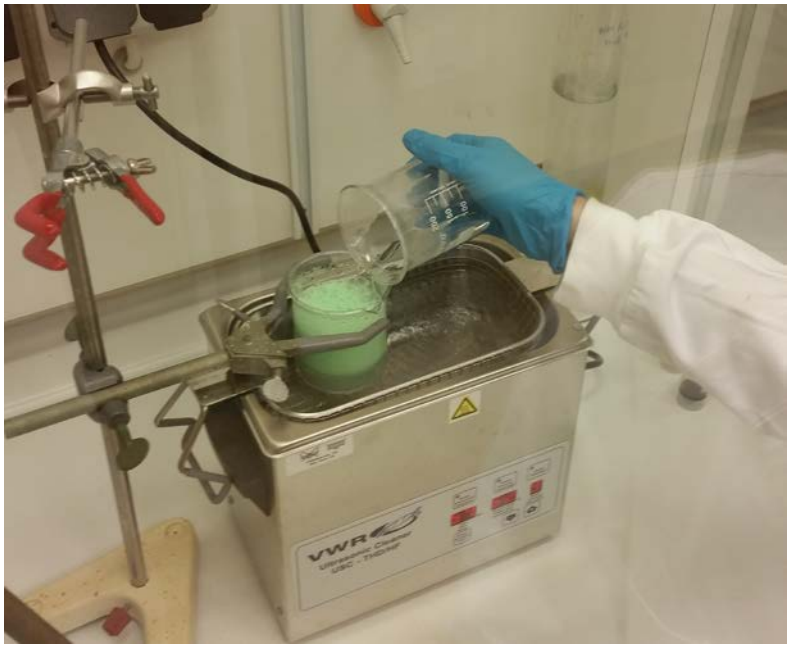

Figure 2. The producing of nanoparticles with ultrasonic water bath

The water bath was stabilised for 15 minutes at 60°C and then the solution was kept in the ultrasonic waterbath for 3 hours. Every hour a 5 ml sample was taken to check the pH, which had to be between 8 and 10 to enable the production of the correct type of nanoparticles of NiO at that temperature.
After the sol-gel process was finished, the samples were kept in the fumehood overnight to sediment as seen in Figure 3. There are two different phases after the sol-gel process, one aqueous on the top and one water rich gel beneath it. The wet gel was filtrated to remove the aqueous part and then washed 3 times by MQ water and dried in an oven at 100°C for 12 h. The aqueous solutions from the sol-gel process were analysed later on using ICP-OES analysis.

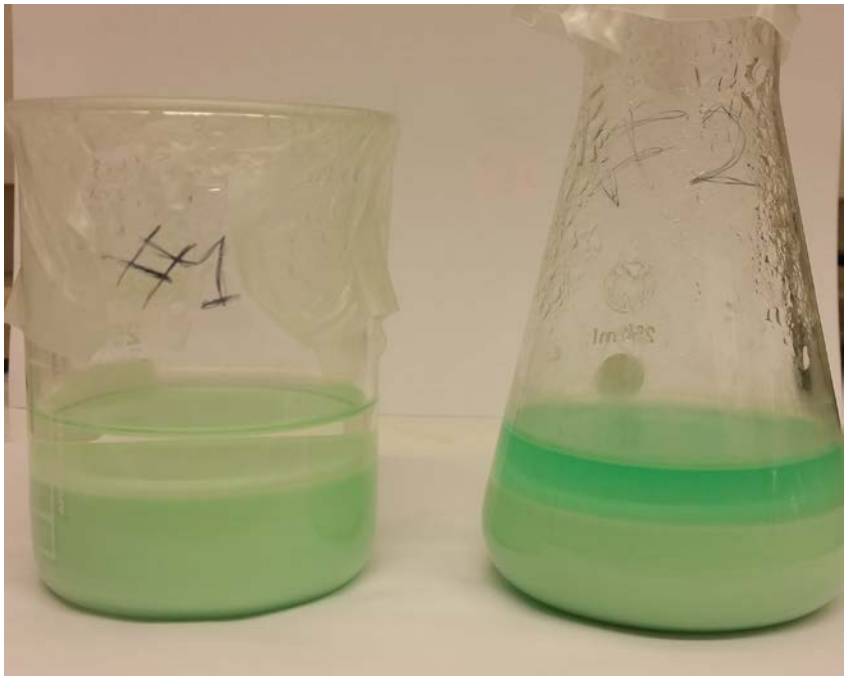

Figure 3. Sample 3 & 2, stratified

Before checking the solid samples in the XRD they were milled. The XRD results showed that there was NaCl in the samples. Due to that the samples were washed with 10 ml of water in the ultrasonic water bath for 15 minutes four times with filtration between the washing and then dried in the oven overnight at 100°C. After this washing procedure XRD analysis showed that all NaCl had been removed.

Figure 4. Sample 1 washed, after drying in oven and after milling

The vortex solutions from all three samples from the sol-gel process were diluted two times and analysed in the ICP-OES.

For the calcination of the produced solid materials three different furnace temperatures: 200°C, 250°C and 300°C, were tested and the samples were in the furnace for 3 hours. Sample 2 was calcinated at 200°C, sample 1 at 250°C and sample 3 at 300°C, Table 4. For sample identification refer to Table 3.

Table 4. Calcination temperatures, time in the furnace and sample number.

Temperature	Time (hour)	Sample
200	1	2
200	2	2
200	3	2
250	1	1
250	2	1
250	3	1
300	1	3
300	2	3
300	3	3

The samples were prepared and made homogeneous by milling and weighed before they were placed in the furnace at each specific temperature. Every hour a sample was removed from the furnace and weighed, showing that there was weight loss after the calcination procedure, Table 5.

Table 5. Calcination temperatures, sample identification, weight before and after calcination.

Temperature	Sample	Weight before calcination (g)	Weight after calcination (g)
200	2	1.0	0.80
200	2	1.0	0.73
200	2	1.0	0.77
250	1	0.8	0.57
250	1	0.8	0.52
250	1	0.8	0.52
300	3	1.0	0.66
300	3	1.0	0.65
300	3	1.0	0.58

Before the heating all samples were green and after the furnace they were black (Figure 5).

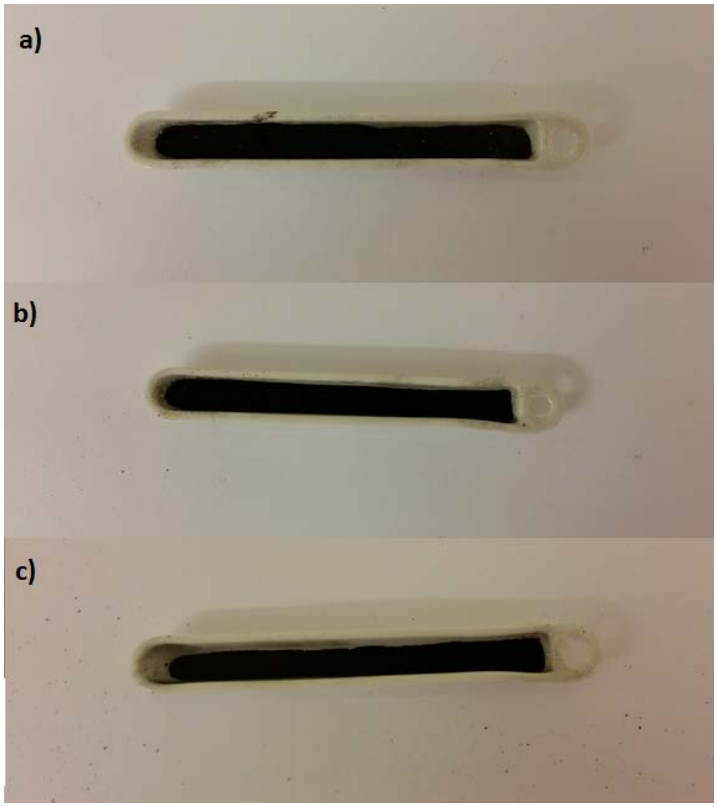

Figure 5. Sample 2 calcinated at 200°C for (a) 1 h, (b) 2 h and (c) 3 h

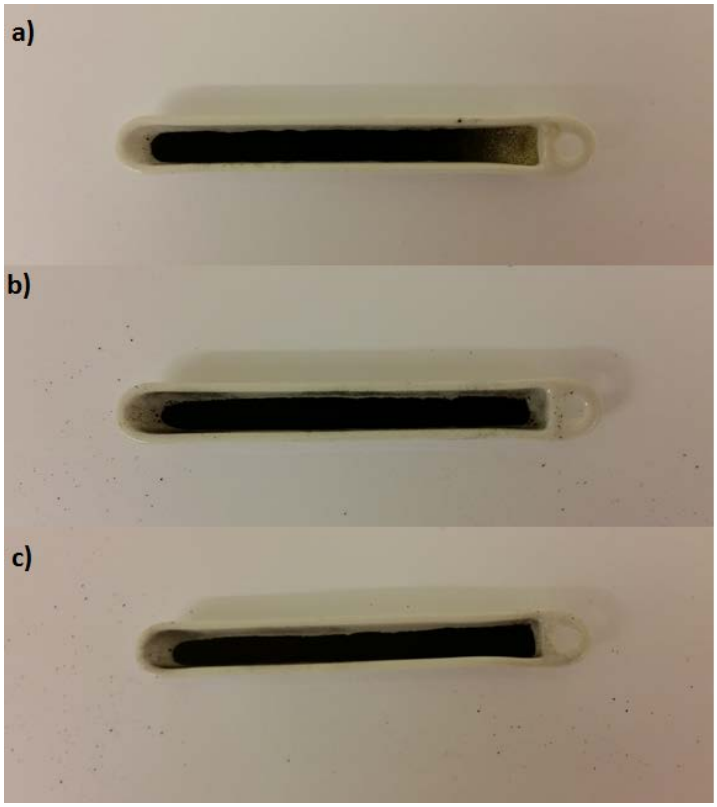

Figure 6. Sample 1 calcinated at 250°C for (a) 1 h, (b) 2 h and (c) 3 h

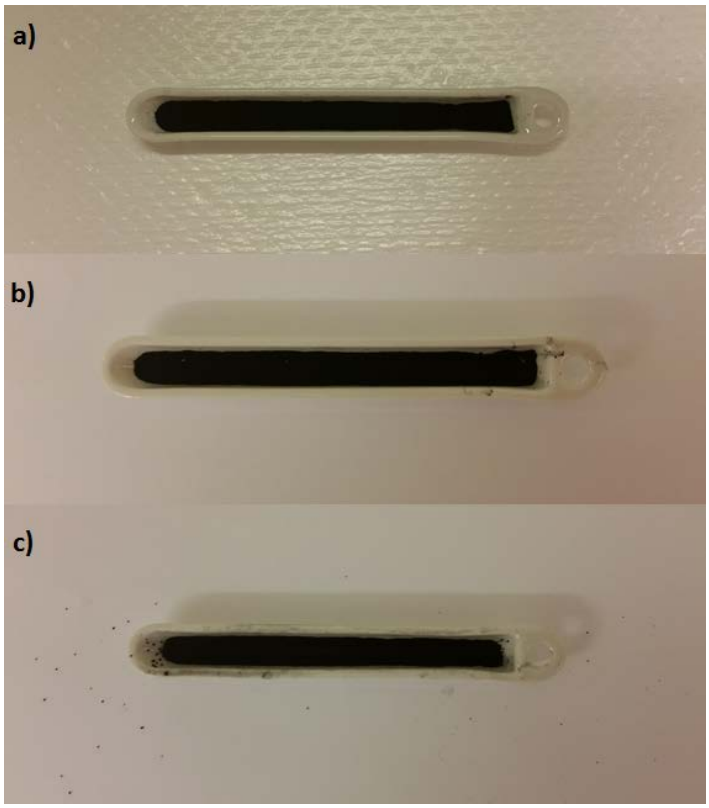

Figure 7. Sample 3 calcinated at 300°C for (a) 1 h, (b) 2 h and (c) 3 h

The particle size of all produced samples was determined using the laser diffraction particle sizer equipment. A small amount of sample was mixed with distilled water and the slurry was kept in the ultrasonic water bath for 15 minutes for mixing. A few drops

of sample slurry was diluted with some distilled water in a special vial for the particle sizer for the measurement.

The calcination process of the $Ni(HCO_3)_2$ particles prepared using the 1.50 M $NaHCO_3$ solution, sample 2, was examined by thermogravimetric analysis (TGA) in the temperature range 25-600°C. Based on the results the calcination parameters 250°C and 3 hours were chosen for an additional sample from the same sol-gel preparation, Figure 8. After the calcination the particles were characterized by XRD, particle sizer and BET surface measurement. The sample taken for the BET analysis was 1.1702 g.

Figure 8. Sample 2 after calcination at 250°C for 3 hours

All particles produced in the sol-gel experiments using 1.00 M, 1.50 M and 1.96 M $NaHCO_3$ respectively and calcined at 300°C for 3 hours were also investigated using FTIR spectrometry. The samples were prepared for the analysis by milling and homogenisation of 1 mg of sample and 100 mg of KBr in a mortar. The homogenised material was pressed at 7,66 MPa for 30 seconds to form a transparent pellet which could be used in the FTIR spectrometer.

Cation adsorption on the formed NiO nano-particles

The cat-ion adsorption experiments were carried out using the nanoparticles produced from sample 2, the 1.5M $NaHCO_3$ solution, and calcination at 250°C for 3 hours. The influence of adsorbent (nanoparticle) amount, concentrations of lead (Pb^{2+}) in the solution and contact time were investigated using 10 ml solutions by variation of these parameters as described in Table 6.

Table 6. Scheme over all samples different concentration, weight and time.

Constant parameters		Variable parameters					
Adsorbant	50 (mg)						
Time	24 h	Concentration (mg/l)	10	25	50	75	100
Concentration	50 (mg/l)						
Time	24 h	Adsorbent Amount (mg)	10	25	50	75	100
Concentration	50 (mg/l)						
Adsorbant	50 (mg)	Time (hour)	2	4	8	16	24

The solution samples from the cation capturing were prepared for the ICP-OES with 2 ml of each sample diluted with 8 ml of 0.5 M HNO_3.

Results & Discussion

ICP results of starting solution and the remaining solution after the sol-gel process

Table 7 presents the results from the ICP-OES analysis of the starting solution (NiMH battery waste leachate) and shows how much nickel it is in the mixed leachate-$NaHCO_3$ solutions after the sol-gel experiments.

Table 7. ICP results

Starting solution		After formation of gel with 1.00 M $NaHCO_3$	After formation of gel with 1.50 M $NaHCO_3$	After formation of gel with 1.96 M $NaHCO_3$
element	g/L	g/L	g/L	g/L
K	0,51	0.048	0.02	0.04
Ni	75,02	1.17	0.03	0.02

XRD and FTIR results of sol-gel samples before calcination

Figure 9 shows the XRD result for sample 3.

As shown in the graph, there are both $Ni(HCO_3)_2$ and NaCl in the samples. NaCl was present in all samples, but the peaks for $Ni(HCO_3)_2$ are not so clear, although it shows that there is traces of crystalline $Ni(HCO_3)_2$ present in the samples. The humps on the background indicate that $Ni(HCO_3)_2$
can be present in amorphous form.

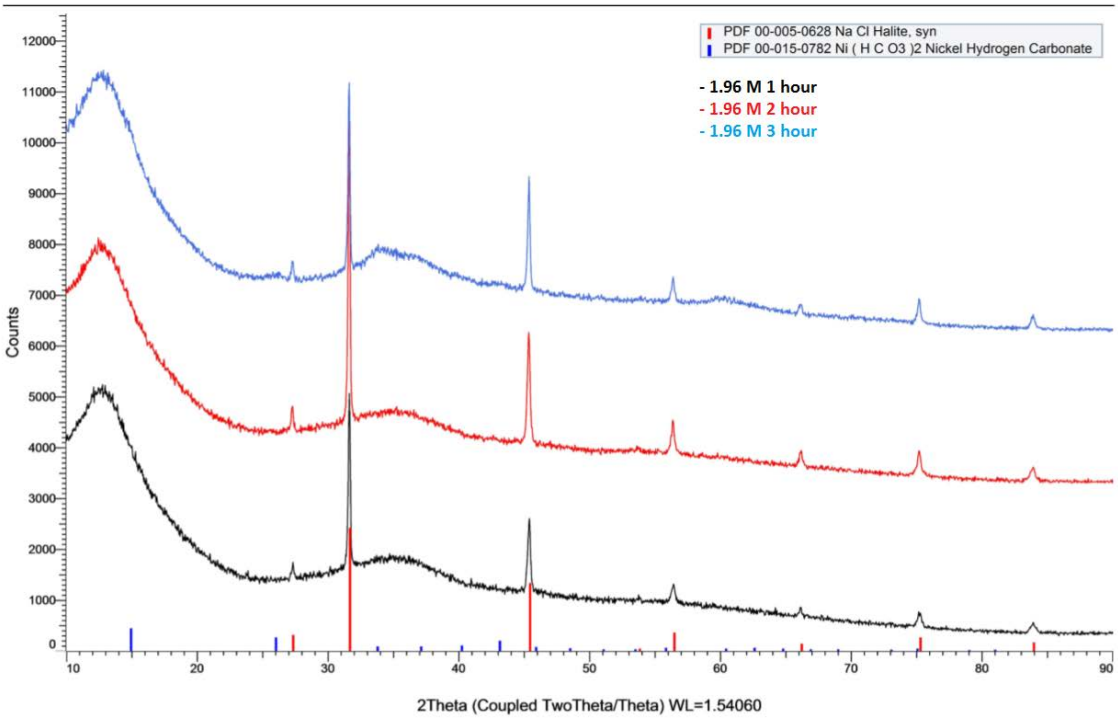

Figure 9. XRD for sample 3 from the sol-gel process, 1-3 hours

Figure 10 shows XRD results for all samples (1-3) produced from the sol-gel process.

NaCl is present in every sample for each concentration and it has very clear peaks. In the graph there are also shown that there are traces of $Ni(HCO_3)_2$ in the samples, but no direct peaks can be detected for either one of the concentrations.

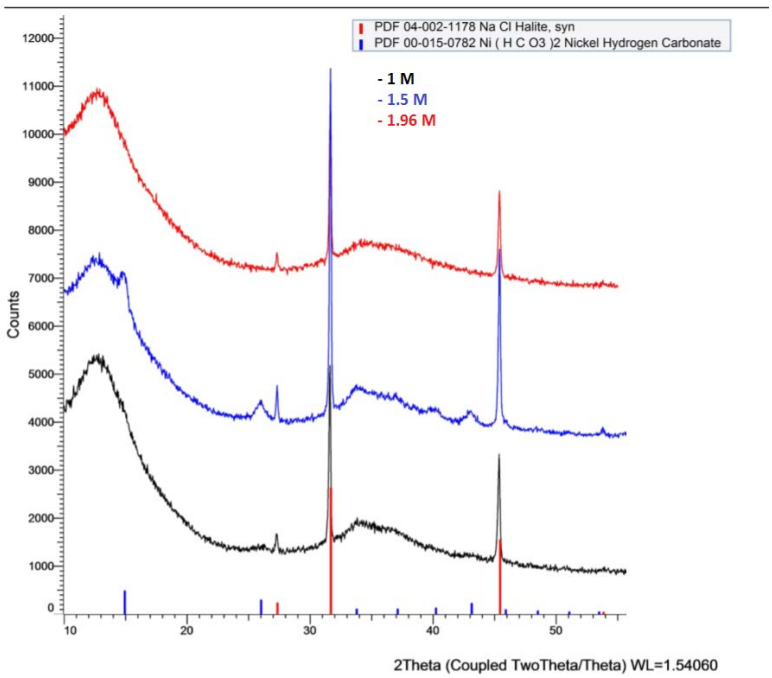

Figure 10. Sample 1-3 produced from the sol-gel process

Figure 11 shows the results from XRD for all samples produced and washed from the sol-gel process.

After washing of the particle samples the amount of NaCl present was clearly reduced as shown in Figure 11. The diffractograms shown in Figure 11 shows that there is crystalline $Ni(HCO_3)_2$ in the samples. The nanoparticles produced using 1.5 M $Na(HCO_3)_2$ are the most crystalline according to the results shown in Figure 11.

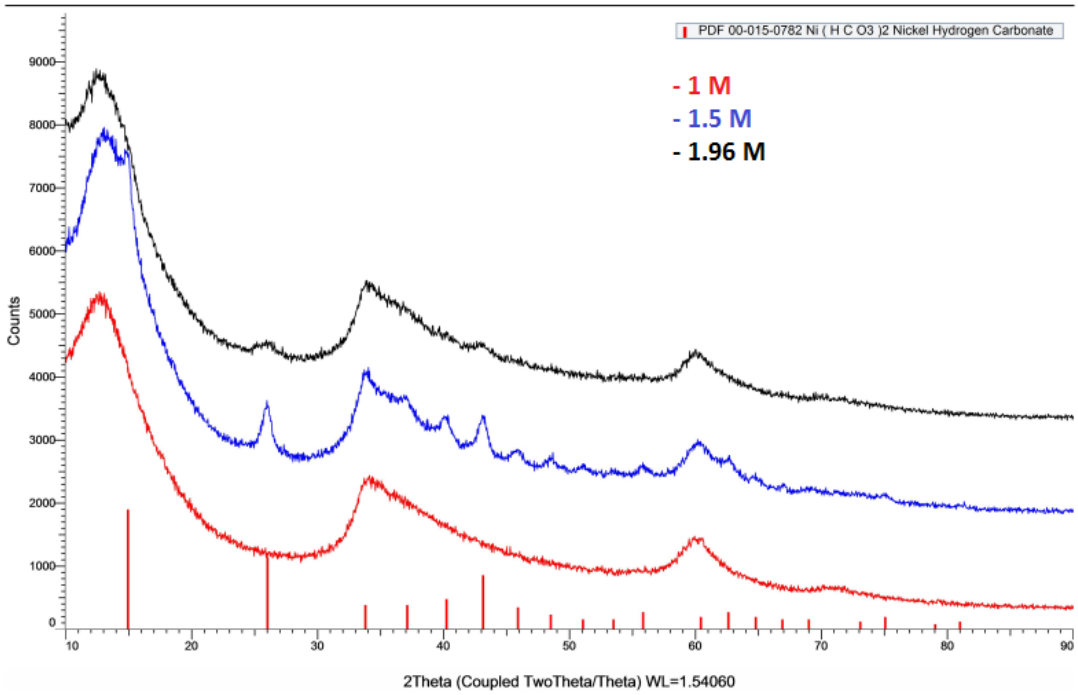

Figure 11. XRD for all washed samples (1-3) from the sol-gel process

Figure 12 shows all results for the washed sol-gel samples from the FTIR analysis.

In the FTIR results the band around 3456 cm^{-1} can be connected to vibrations of hydroxyl groups. At 1543cm^{-1} the band is attributed to the H-OH vibration. The three weaker bands at 824, 1061 and 1459 cm^{-1} are characteristics of carbonate ions and the band at 680 cm^{-1} can be associated with Ni-OH bending vibrations. This shows that there are probably ($Ni(HCO_3)_2$) present in all samples, and that the particles produced using $Na(HCO_3)_2$ in the concentrations 1.5 M and 1.96 M are similar to those produced using 1 M sodium bicarbonate solution.

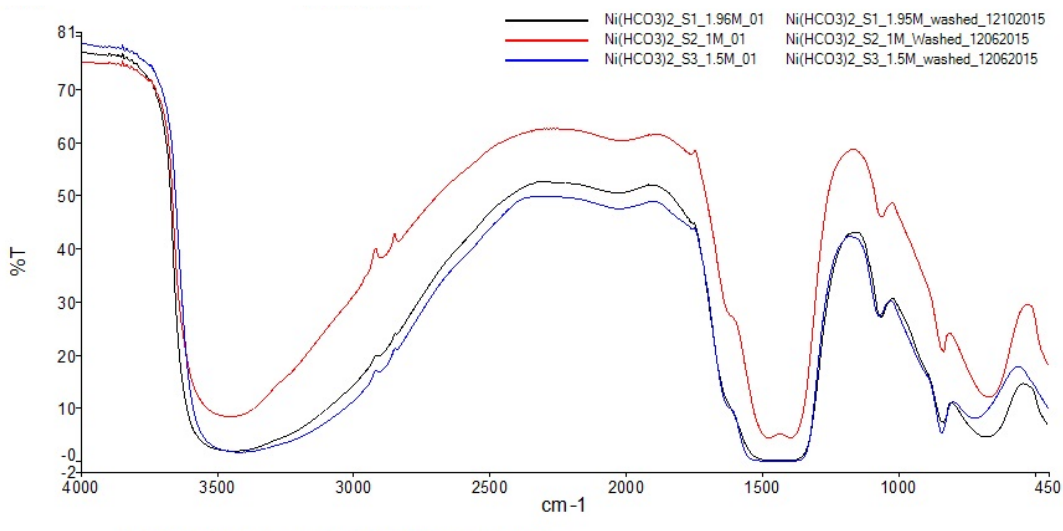

Figure 12. FTIR on all washed sol-gel samples (1-3)

Comparing XRD and FTIR spectrometry results for all three nanoparticle materials produced in the sol-gel experiments gives a good insight of the chemical compounds in the samples. The results clearly show that all samples are mainly composed of nickel hydrogen carbonates and production of NiO nanostructured particles should be possible to achieve by a simple calcination process using these sol-gel products.

Recovery efficiency of Ni from solution into nanoparticles

Table 8 shows the Nickel recovery efficiency for each concentration of the $NaHCO_3$ solution. The Nickel recovery efficiency was calculated by equation [1].

Due to table 7, sample 3 should have the highest nickel recovery efficiency, but the volumes of the final solutions from the sol-gel process aren't exactly the same. And that explains why sample 2 have the highest nickel recovery efficiency.

The nickel recovery efficiency results shows that sample 2 and sample 3 had the highest recovery efficiencies. The 1.50 M sample had the highest recovery and used less chemicals, it was considered the most suitable one to continue further experiments on.

Table 8. Nickel recovery efficiency

Sample	Concentration of NaHCO3	Nickel recovery efficiency
1	1.00 M	92%
2	1.50 M	99%
3	1.96 M	99%

Particle size of sol-gel samples

Table 9 shows the average particle size of the produced nanoparticle samples. The particle size is connected to the concentration of $NaHCO_3$ used in the sol-gel experiment, i.e., the highest concentration gives the smallest size of the particles.

For the capturing of cations, it is more suitable with a smaller particle size since it gives a larger surface area per weight unit.

Table 9. Average particle size

Sample	Concentration of NaHCO3	Average particle size (nm)
1	1.00 M	3000
2	1.50 M	2940
3	1.96 M	879

Thermal Analysis of $Ni(HCO_3)_2$

Figure 13 shows at which temperatures sol-gel samples start losing weight and reactions occur.

There is a 13% weight loss around 200°C, followed by a small loss at 247°C. The reaction is continued and completed at 400°C, with a weight loss of about 46%.

The temperatures for the calcination of the nanoparticles produced in the sol-gel process was thereby determined around the reaction temperatures for the sample, 200°C, 250°C and 300°C. 300°C was chosen instead of 400°C since there is still a reaction at that temperature and it is having a lower energy requirement.

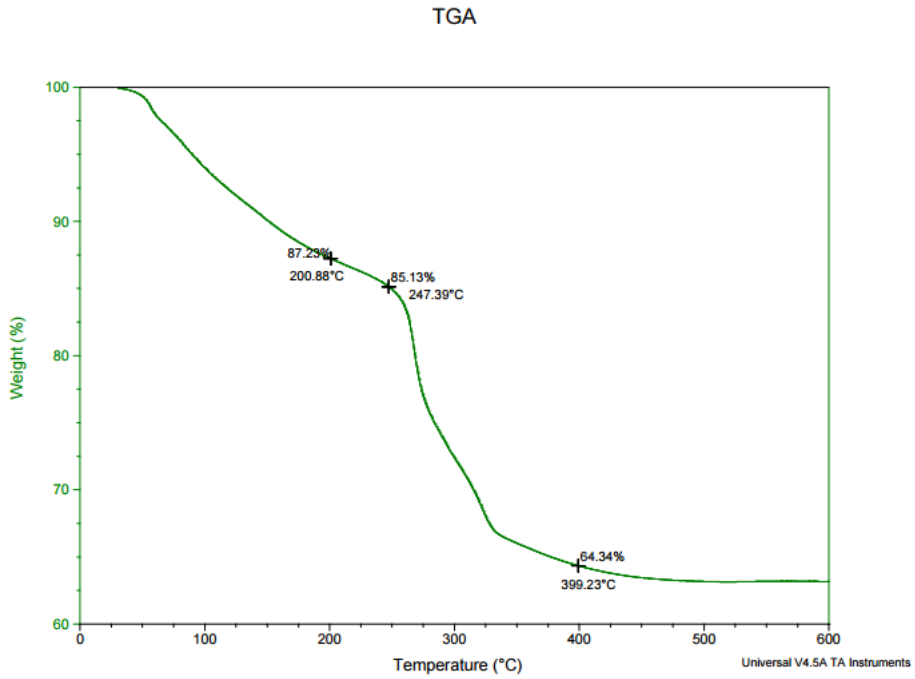

Figure 13. TGA result of NiHCO

XRD and FTIR of NiO particles

Table 10 shows the crystallite size, the size of a single crystal in the powder form, for the calcinated samples.

As seen in Table 10, the crystallite size is very similar for 2 and 3 hours at 250°C and the same for 2 and 3 hours at 300°C.

For the sample treated for 1 hour at 250°C the particles are not crystallized, therefore there is no measurement for the average crystallite size at that time and temperature.

Table 10. Crystallite size for calcinated samples

Temerature	Time	Average Crystallite size
250	1	-
250	2	4.4 nm
250	3	4.5 nm
300	1	4.5 nm
300	2	5.4 nm
300	3	5.4 nm

Figure 14 gives the XRD results for calcinated sample 2 after 1-3 hours at 200°C.

After calcination at 200°C the XRD results shows that there is $Ni(HCO_3)_2$ and two types of NiO in the sample material at that temperature.

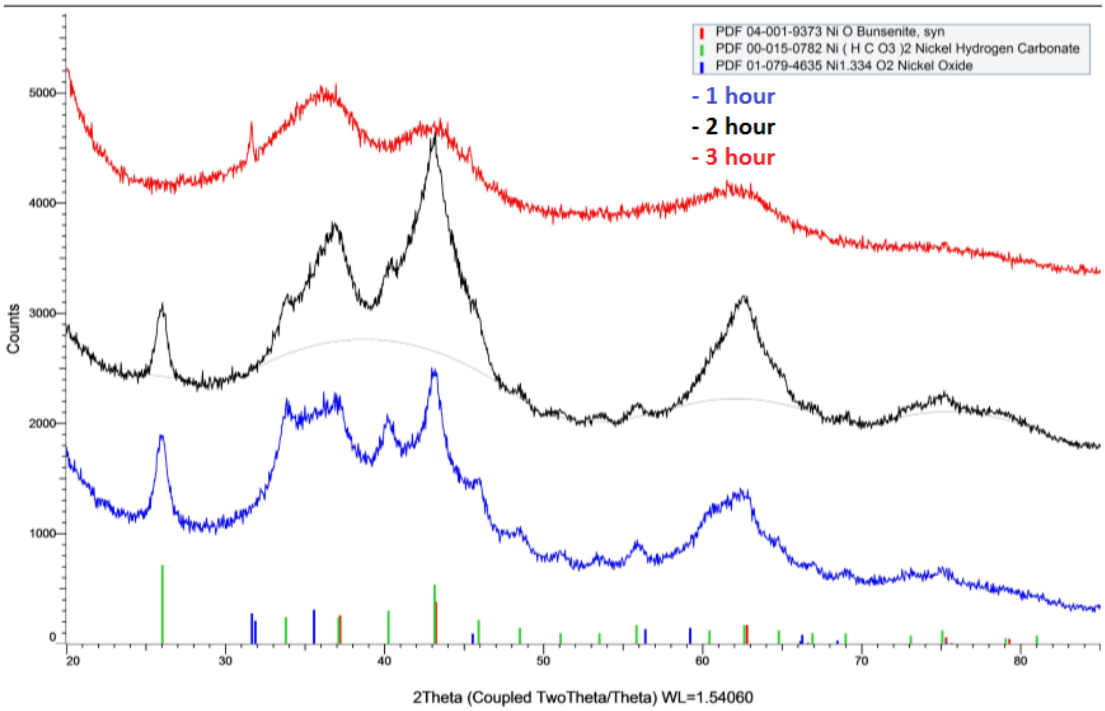

Figure 14. Calcinated sample 2 at 200°C 1-3 hours

Figure 15 shows the results of XRD for calcinated sample 1 for 1-3 hours at 250°C.

In the XRD results for sample 1 after 1 hour in the furnace, the peaks are very weak and does not match NiO, compared to 2 and 3 hours in the furnace. This could be because there is not enough time for the first hour at 250°C for the sample to crystallite. Both samples treated for 2 and 3 hours at 250°C are very similar, both in the XRD results and in crystallite size, table 10. There is hardly any difference between them.

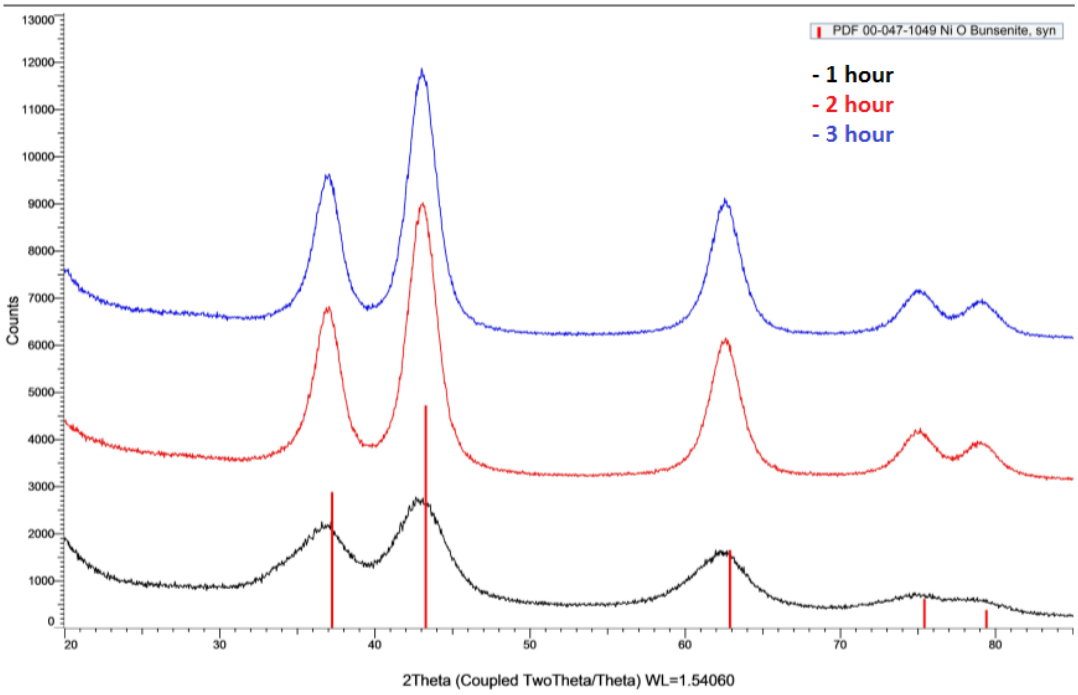

Figure 15. XRD for calcinated sample 1 at 250 °C 1-3 hour

Figure 16 shows the XRD results after calcination at 300°C for sample 3 for 1-3 hours.

At 300°C there are no big difference between 1-3 hours. All three of them contain NiO. Looking at table 7 the last two are more crystallized and have the same size, 2 and 3 hours are more preferable.

At 250°C, Figure 15, and at 300°C, Figure 16, there is only NiO present in the sample, which makes these two temperatures most interesting to continue with.

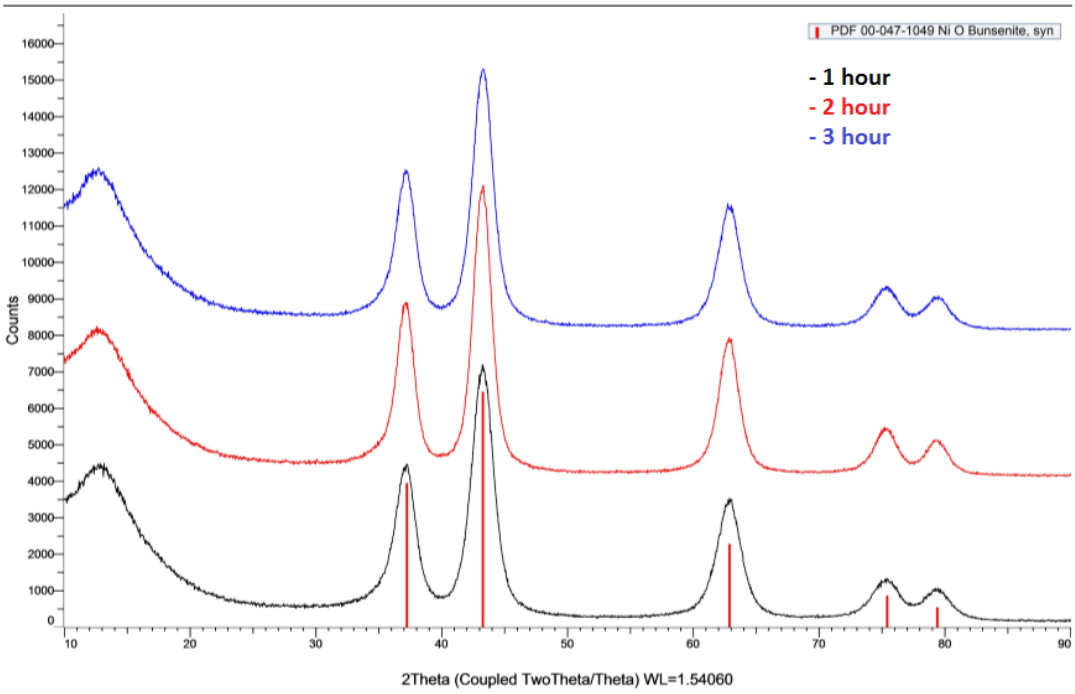

Figure 16. XRD for calcinated sample 3 at 300°C for 1-3 hours

Figure 17 shows FTIR results for washed sample 2 and calcinated sample 2.

In the FTIR results the band region of 600-700 cm-1 is assigned to Ni-O stretching vibration. At 3440 cm-1 the broad absorption is attributed to the band O-H stretching vibrations and at 1635 cm-1 is assigned to the H-O-H bending vibrations. The bands in the region of 1000-1500 cm-1 are assigned to the O-symmetric and assymetric stretching vibrations and the C-O stretching vibration.

Washed sample 2 contains $Ni(HCO_3)_2$ which matches these vibrations in the FTIR for that sample. The spectrum of the calcinated sample 2 also partly matched with the same vibrations but it has some deviations that match the NiO stretching vibrations.

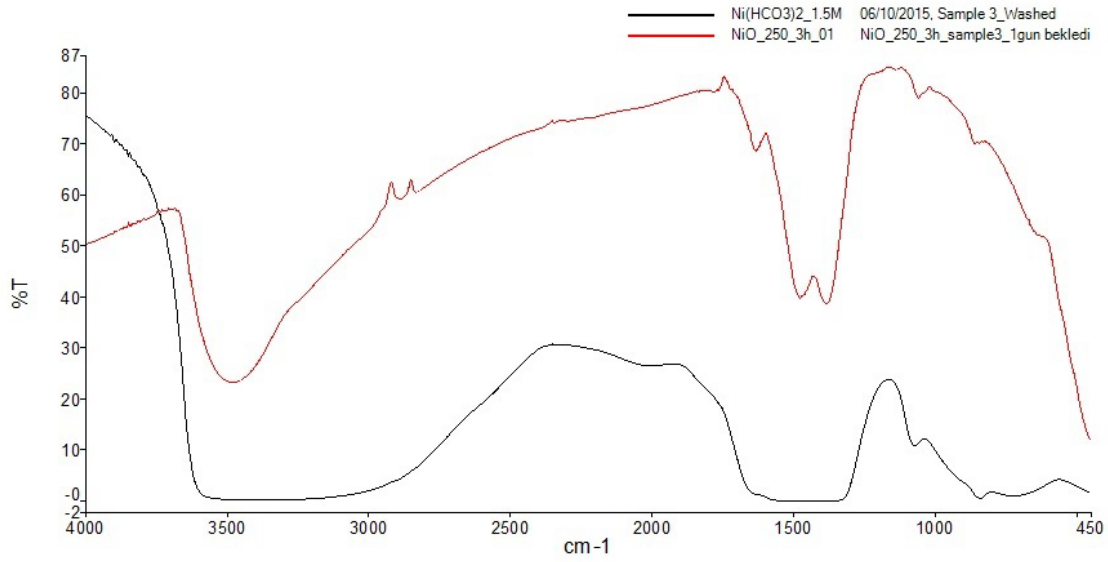

Figure 17. FTIR for washed sample 2 and calcinated sample 2 at 250°C

Characterization of the produced NiO particles

Figure 18 shows a) 3 hours at 300°C, b) 2 hours at 250°C and for c) 3 hours at 250°C.

The particle morphology, size distribution and specific surface areas of the produced NiO particles were investigated using SEM, laser diffraction particle size determination and BET surface area characterization methods. The results showed that calcination at 300°C for 3 hours resulted in agglomeration of the nanoparticles (Figure 18 a) whereas a temperature of 250°C gave more distinct particle structure. However, the particles that were calcinated at 250°C for 2 hours (Figure 18 b) also showed some agglomeration and the particles seem to be somewhat bigger than those produced at 250°C for 3 hours.

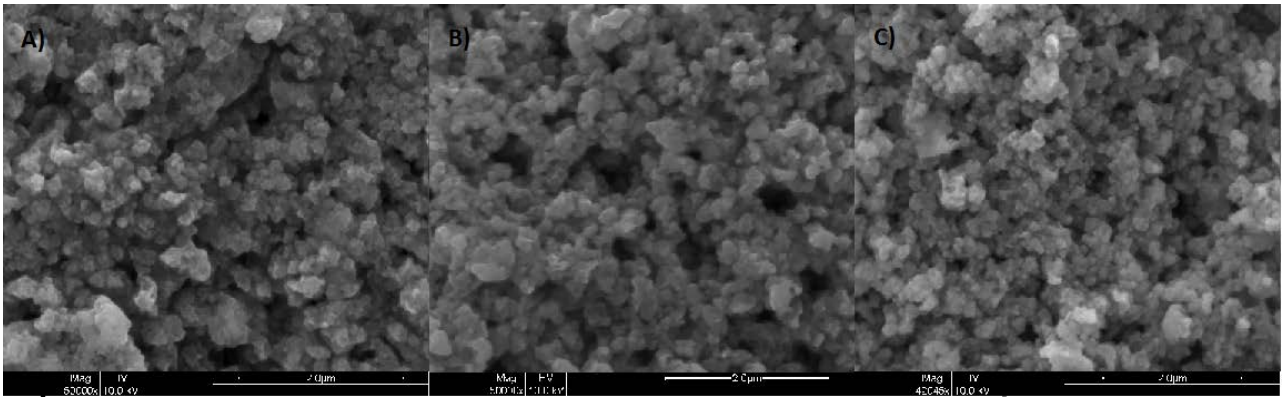

Figure 18. SEM images of sample 2 at 300°C for 3 hours and at 250°C for 2 and 3 hours.

Table 11 presents the results for the average particle sizes for the calcinated samples.

For the average particle size there is almost no change between the sample treated at 250°C for 2 hours that treated for 3 hours. However, the sample treated for 1 hour at 250°C had a significantly bigger particle size, compared to the other samples treated at that temperature. This sample could be agglomerated since it has not been in the furnace long enough. At the same time there are two different results for 250°C, one result is 273 nm while the other one is about five times bigger. This could also be due to agglomerated particles and differences within the sample material.
There is a 200 nm difference between the particles that have been calcinated for1 hour, 2 hours and 3 hours at 300°C. There is a possibility that all these samples are agglomerated since they do not deviate much from each other and have very large particle sizes.

Table 11. Average particle size for calcinated samples

Temperature	Time	Average particle size
250	1	765 nm
250	2	275 nm
250	3	273 nm
300	1	1956 nm
300	2	1789 nm
300	3	1715 nm

Table 12 gives the results from the BET and table 9 shows the average particle sizes for the calcinated samples.

The result from BET shows that calcinated sample 2 at 200°C has a big surface area, which is good for the capturing of cations. It also shows the calculated nanoparticle size by the surface area of the sample.

Table 12. BET results

Surface area	178.9 m2/g
Calculated Nanoparticle size	5 nm

The SEM results and average particle sizes of the NiO particles show that the most suitable temperature and time for the calcination are 250°C and 3 hours to obtain the finest particles. The material calcinated in these settings has the best structure of the particles and smallest and is therefore the best choice for removal of heavy metals.

Adsorption isotherms for Pb capturing as a function of time, lead concentration and adsorbent dosage.

The adsorption capacity and removal efficiency obtained while varying three different parameters are shown in Figure 19-21.

Equation [2] was used to calculate the adsorption capacity and equation [1] to calculate the removal efficiency for each parameter.

In Figure 19 the results are presented by a graph with adsorbent dosage as the variable parameter, under 50 mg/l Pb concentration and 24 h duration conditions.
The results show that the lead removal efficiency is varying with the absorbent dosage. The catalytic effect of NiO nanoparticles and their agglomeration tendency can cause these changes. The removal efficiency is the highest (85%) for 0.075 g of nano particles added to the 10 ml lead containing water sample and this indicates that that amount of adsorbent is the most efficient for removal efficiency, at these constant parameters. This means 7.5 grams of nano particles per liter of water.

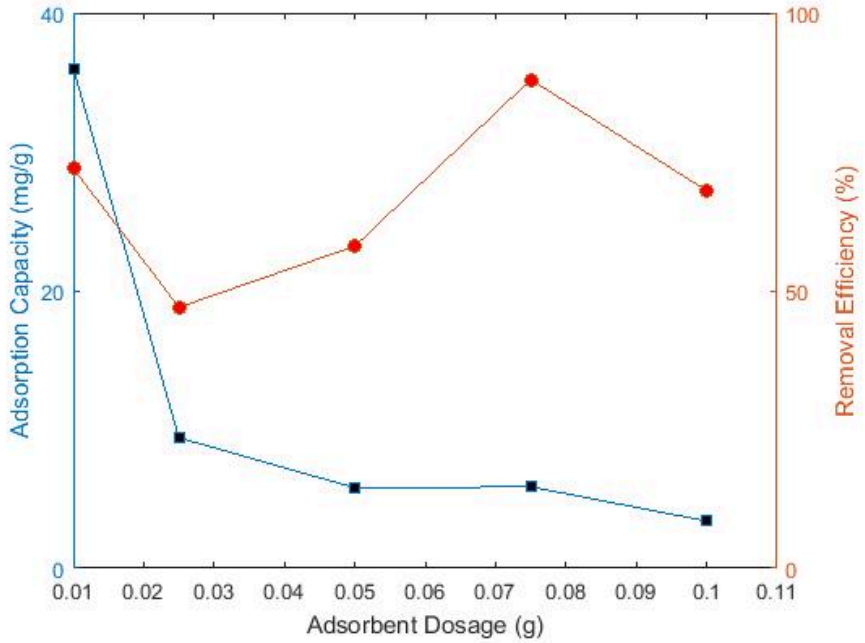

Figure 19. Adsorption capacity and Removal efficiency versus Adsorbent Dosage

Figure 20 shows the results from ICP-OES with time as a variable parameter, using 50 mg/l Pb concentrated solution and 50 mg NiO absorbent.

In this graph the curve for the adsorption capacity and the removal efficiency are the same.
Both the concentration of Pb-ions and adsorbent dosage were constant during the experiment.

No adsorption equilibrium is reached.

The curve is decreasing slowly between 2 to 4 hours and 16 to 24 hours. A big deviation is seen at 8 hours, the curve first heavily decreases from 4 hours to 8 hours, and then increase to 16 hours. The pH for the 8 hour sample could be very high or low at that point since there are very low values for both adsorption capacity and removal efficiency, it is clearly interfering with the results.
The highest values for adsorption capacity and removal efficiency are in the beginning of 2 hours, with 9.8 mg/g and respectively 98% and the lowest at 8 hours around 10%.

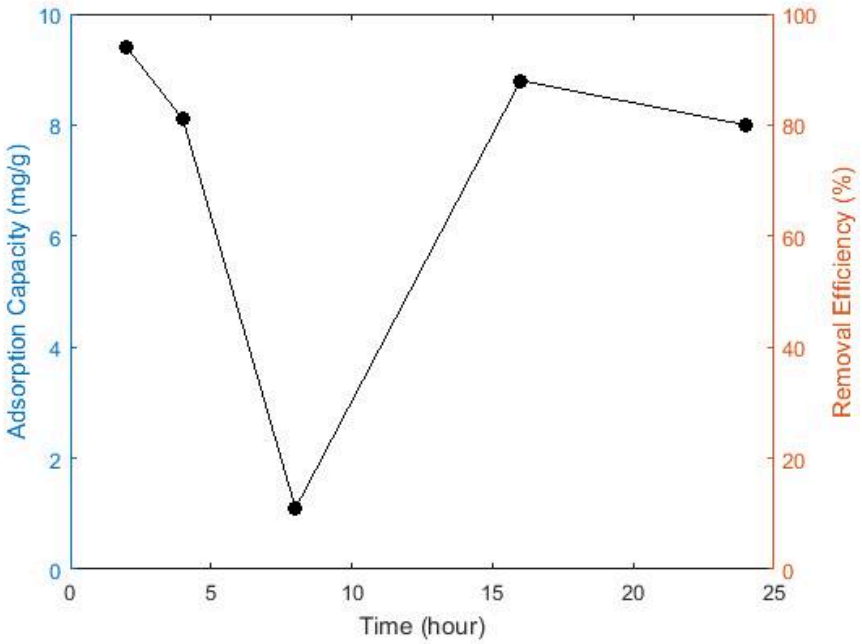

Figure 20. Adsorption capacity versus Time

Figure 21 shows the results from ICP-OES by a graph with concentration of lead as a variable parameter, using 50 mg NiO absorbent for 24 h duration.

The removal efficiency is the highest for 100 mg/l, 80%, and the lowest for 75 mg/l, 42%. From 25 mg/l to 75 mg/l the curve decreases for the removal efficiency. This could be because of the pH and it affects the removal efficiency. Unfortunately, doing more research and experiments about this theory was not possible, due to lack of time. For further research in this area it could be an interesting topic. This may also improve the results of this experiment.

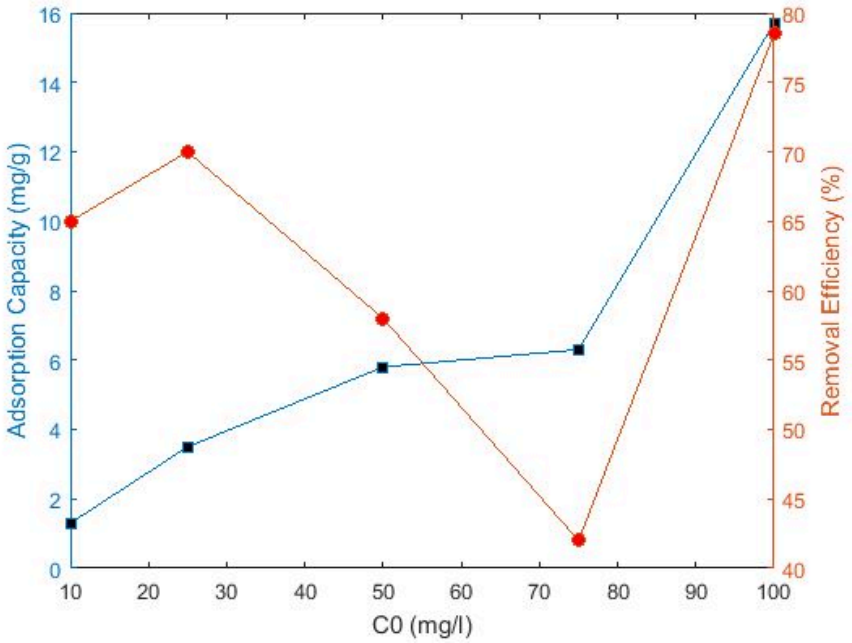

Figure 21. Adsorption capacity versus Concentration

Since the adsorption of Pb^{2+} is very dependent on the pH in the solution, it is of great importance to adjust the solution pH so that the adsorption of the heavy metal is efficient and not affected by this [12].
In every graph there are values which deviate, for example in Figure 21, at 8 hours. This could be because of the pH change in the sample over time and it affects the adsorption [9]. At pH<7 there could be a lot of H^+ that reacts with the NiO and at pH>7 the negatively charged OH^- are reacting with the Pb^{2+} [10], this requires further study.

As shown by the results, the cation capturing experiment was successful.

Conclusions

In this study the producing of fine advanced nanoparticles of Nickel from Ni-MH battery waste solution with $NaHCO_3$ was successful and gives opportunity for further use and research.

Different concentrations of $NaHCO_3$ were used in the production of nanoparticles to study the best suitable parameter settings to produce good adsorbent particles for the cat-ion capturing. The NiO nanoparticles were characterized using following methods; XRD, FTIR, Particle sizer and ICP-OES. By comparing these different samples compounds, chemical compositions and the nickel recovery efficiency from the recycled nickel solution for each concentration, the best settings for the sol-gel formation was determined and it gave about 98% Ni recovery.

To determine the calcination temperature for the primary particles TG analysis was performed and the calcined sample was analysed by XRD, FTIR, SEM, Particle sizer and BET to find out more information about the surface area, microstructure and nanoparticle size obtained at different temperatures. The most appropriate temperature could be determined due to the chemical composition of calcinated samples (NiO), and it was 250°C for 3 hours.

These analyses showed that the process of producing nanoparticles was successful since there was NiO in the calcinated samples.

After analysing the produced samples and deciding which concentration of $NaHCO_3$ and which calcination temperature was the most suitable to continue further study with, the next step, cation capturing, could continue.
For the cat-ion capturing the NiO nanoparticle sample was shaken with an aqueous solution of Pb^{2+} at different Pb^{2+} concentrations, adsorbent dosages and times, to see how these parameters affects the adsorption capacity and removal efficiency.

The results from this study are successful, but due to time constraint, every experiment was only done once. Hence, they need to be repeated to get a more solid confirmation of the results.

The results for lead ion adsorption capacity and removal efficiency shows that nickel oxide works for cation capturing and the study was successful. The removal efficiency obtained in these preliminary experiments was about 80%, which shows that further development of the suggested nanoparticle production process is worth pursuing.

References

1. Batteriföreningen 2016-01-22: http://batteriforeningen.se/laddningsbara/nicdnimh/oversikt-vanligt-forekommande-nimh-batterier/

2. Santos, V.E.O, Celante, V.G. Lelis, M.F.F Freitas, M.B.J.G (2012) *Chemical and electrochemical recycling of the nickel, cobalt, zinc and manganese from the positives electrodes of spent Ni-MH batteries from mobile phones*

3. Batteriguiden 2016-01-22: http://www.stgeorge.se/batteriguiden

4. Naturvårdsverket 2016-01-22: *http://www.naturvardsverket.se/*

5. Larsson, K. Binnemans, K. (2014) *Selective extraction of metals using ionic liquids for nickel metal hydride battery recycling*

6. Metal prices from 2016-01-22: http://www.metal-supply.se/

7. Hua, M. Zhang, S. Pan, B. Zhang, W. Lv, L. Zhang, Q. (2012)*Heavy metal removal from water/wastewater by nanosized metal oxides: A review*

8. Kemikalieinspekionen 2016-01-22 http://www.kemi.se/

9. He, Y. Zhang, L. Wang, R. Li, H. Wang, Y. (2012) *Loess clay based copolymer for removing Pb(II) ions*

10. Singh, S. Barick, K.D. Bahadaur, D. (2011) *Surface engineered magnetic nanoparticles for removal of toxic metal ions and bacterial pathogens*

11. Huang, K. Li, J. Xu, Z. (2010) *Characterization and recycling of cadmium from waste nickel-cadmium batteries*

12. Guo, X. Du, B. Wei, Q. Yang, J. Hu, L. Yan, L. Xu, W. (2014) *Synthesis of amino functionalized magnetic graphenes composite material and its application to remove Cr(VI), Pb(II), Hg(II), Cd(II), and Ni(II) from contaminated water*

13. Erdem, E. Karapinar, N. Donat, R. (2004) *The removal of heavy metal cations by natural zeolites*

14. Reuter, H. (1991) *Sol-gel processes*

15. Suryanarayana, C. (1998) *X-Ray Diffraction A Practical Approach. 1.1 X-Rays.*

16. Particle Size Analyser 2015-07-20 http://www.brookhaveninstruments.com/nanobrook-90plus

17. Wang, Y. Petrova, V. (2012) *Nanotechnology research methods for foods and bioproducts. Chapter 6. Scanning Electron Microscope*

18. Stanley, H. Thornton, T. (2002) *What is "BET Surface Area" and How Does It Affect the Performance of a Battery?*

19. Chabert, P. (2011) *Chapter 3. Incutively Coupled Plasmas*

20. Harris, D.C. (2007) *Quantitative Chemical Analysis*

21. Larsson, K. (2012) Hydrometallurgical Treatment of NiMH Batteries, PhD Thesis, Chalmers University of Technology, Göteborg, Sweden (ISBN: 978-91-7385-722-2)